A Comparison of the Influences of Alkoxide and Thiolate Ligands on the Electronic Structure and Reactivity of Molybdenum(3+) and Tungsten(3+) Complexes. Preparation and Structures of $M_2(O^tBu)_2(S^tBu)_4$, $[Mo(S^tBu)_3((NO)]_2$, and $W(S^tBu)_3(NO)(py)$

Malcolm H. Chisholm,* Ernest R. Davidson,* John C. Huffman, and Kristine B. Quinlan

Contribution from the Department of Chemistry and Molecular Structure Center, Indiana University, Bloomington, Indiana 47405

Received April 6, 2000

Abstract: $M_2(O^tBu)_6$ compounds (M = Mo, W) react in hydrocarbon solvents with an excess of ^{t}BuSH to give $M_2(O^tBu)_2(S^tBu)_4$, red, air- and temperature-sensitive compounds. ^{1}H NMR studies reveal the equilibrium $M_2(O^tBu)_6 + 4^t$BuSH ⇌ $M_2(O^tBu)_2(S^tBu)_4 + 4^t$BuOH proceeds to the right slowly at 22 °C. The intermediates $M_2(O^tBu)_4(S^tBu)_2$, $M_2(O^tBu)_3(S^tBu)_3$, and $M_2(O^tBu)_5(S^tBu)$ have been detected. The equilibrium constants show the M−O^{t}Bu bonds to be enthalpically favored over the M−S^{t}Bu bonds. In contrast to the $M_2(O^tBu)_6$ compounds, $M_2(O^tBu)_2(S^tBu)_4$ compounds are inert with respect to the addition of CO, CO_2, ethyne, ^{t}BuC≡CH, MeC≡N, and PhC≡N. Addition of an excess of ^{t}BuSH to a hydrocarbon solution of $W_2(O^tBu)_6(\mu$-CO) leads to the rapid expulsion of CO and subsequent formation of $W_2(O^tBu)_2(S^tBu)_4$. Addition of an excess of ^{t}BuSH to hydrocarbon solutions of $[Mo(O^tBu)_3(NO)]_2$ and $W(O^tBu)_3(NO)(py)$ gives the structurally related compounds $[Mo(S^tBu)_3(NO)]_2$ and $W(S^tBu)_3(NO)(py)$, with linear M−N−O moieties and five-coordinate metal atoms. The values of ν(NO) are higher in the related thiolate compounds than in their alkoxide counterparts. The bonding in the model compounds $M_2(EH)_6$, $M_2(OH)_2(EH)_4$, $(HE)_3M{\equiv}CMe$, and $W(EH)_3(NO)(NH_3)$ and the fragments $M(EH)_3$, where M = Mo or W and E = O or S, has been examined by DFT B3LYP calculations employing various basis sets including polarization functions for O and S and two different core potentials, LANL2 and relativistic CEP. BLYP calculations were done with ZORA relativistic terms using ADF 2000. The calculations, irrespective of the method used, indicate that the M−O bonds are more ionic than the M−S bonds and that E pπ to M dπ bonding is more important for E = O. The latter raises the M−M π orbital energies by ca. 1 eV for $M_2(OH)_6$ relative to $M_2(SH)_6$. For $M(EH)_3$ fragments, the metal d_{xz},d_{yz} orbitals are destabilized by OH pπ bonding, and in $W(EH)_3(NO)(NH_3)$ the O pπ to M dπ donation enhances W dπ to NO π* back-bonding. Estimates of the bond strengths for the M≡M in $M_2(EH)_6$ compounds and M≡C in $(EH)_3M{\equiv}$CMe have been obtained. The stronger π donation of the alkoxide ligands is proposed to enhance back-bonding to the π* orbitals of alkynes and nitriles and facilitate their reductive cleavage, a reaction that is not observed for their thiolate counterpart.

Introduction

What are the essential differences in the ligation of alkoxides and thiolates to metal centers? Why does nature sometimes elect to employ sulfur and in other times oxygen donor ligands in metalloenzymes? While probably every chemist would offer an answer to the above and there would likely be some common ground in the responses, it is probably fair to say that there is no simple and unique answer that is universally correct. Metal ions can be classified as hard or soft and paired with their respective hard (oxygen) or soft (sulfur) ligands,[1] but even this is complicated by the fact that a given metal can be viewed as hard or soft depending upon its oxidation state and the nature of its ancillary ligands. Iron(II) may be viewed as soft and iron(III) as hard, but this classification is as greatly influenced by spin state as it is by formal oxidation state, and the former is decided by the ancillary ligand environment. A metal such as tungsten is oxophilic and in its high oxidation states can be viewed as hard.[2] However, in its low oxidation states it is soft.[2] But what of tungsten in its middle oxidation states? Does it prefer a soft ligand such as a thiolate or a hard ligand such as an alkoxide? In closely related compounds how do the bonding and reactivity compare? This last question is difficult to answer because there are very few related series. To give a few examples from the recent literature and the thinking therein, we note the following.

In 1995, Bergman and co-workers[3] reported that the addition of *p*-thiocresol to the phenoxide complex shown in eq 1 led to

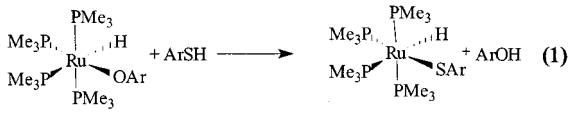

(1)

quantitative formation of the arylthiolate at room temperature. They argued that the Ru−S bond was stronger than the Ru−O bond because of the soft Ru(2+) center and its favorable coordination to the soft sulfur bond. Also the reaction is driven to the right by the difference in E−H bond dissociation energies

(1) Pearson, R. G. *J. Am. Chem. Soc.* **1963**, *85*, 3533.

(2) Chisholm, M. H.; Folting, K.; Kramer, K. S.; Streib, W. E. *Inorg. Chem.* **1998**, *37*, 1549.

(3) Burn, M. J.; Fickes, M. G.; Hollander, F. J.; Bergman, R. G. *Organometallics* **1995**, *14*, 137.

10.1021/ja001208n CCC: $20.00 © 2001 American Chemical Society
Published on Web 09/07/2001

since in PhSH the S−H bond is weaker than the O−H bond by 3 kcal mol^{-1}.[4]

Estimates of M−X bond strengths by studies of equilibria of the type $L_nM-X + H-Y \rightleftharpoons L_nM-Y + H-X$ were further supported by the calorimetric studies of Nolan et al.[5] on reactions shown in eqs 2 and 3**.**

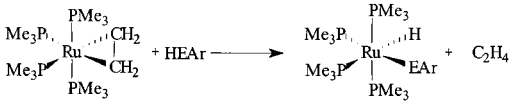

(2)

$$Cp^*Ni(PEt_3)(Otolyl) + tolylSH \rightarrow Cp^*Ni(PEt_3)(Stolyl) + tolylOH \quad \textbf{(3)}$$

Reaction 2 was found to be exothermic by ca. 24 kcal mol^{-1} for a wide range of aryl groups when E = S relative to E = O. Thus, even allowing for the stronger ArO−H bonds compared to ArS−H bonds, the Ru−S bond can be viewed to be favored by ca. 20 kcal mol^{-1}. Also, for related structures, the Ru−P bond distances *trans* to Ru−EAr bonds revealed that Ru−P is longer when *trans* to the Ru−S bond, indicating the stonger σ donor influence (*trans*-influence) of the Ru−SAr bond.[6] Similarly, for a series of complexes of the form *cis*-[IrH(X)-$(PMe_3)4]^+[PF6]^-$, where X = OH, SH, OCH_3, CH_2OH, and H, which have been crystallographically characterized, the *trans*-influence series H > CH_2OH > SH > OCH_3 > OH was observed.[7]

For reaction 3, the $\Delta H°_{reaction} = -14$ kcal mol^{-1}, while for reaction 1 a calorimetric study gave $\Delta H° = -24$ kcal mol^{-1} as expected from the studies of reaction 2.

All of the above have metals with filled d_π orbitals for which E p_π to M d_π bonding would be destabilizing. In this regard it is interesting to compare the 1998 report by Wigley et al.[8] on the formally d^0 Ta(5+) complex shown in **I** below. The structures were reported for both the O^{t}Bu and S^{t}Bu complexes.

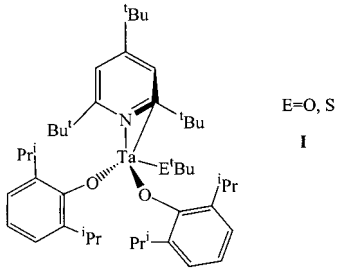

E=O, S

I

The Ta−C bond distance is significantly longer in the thiolate complex (2.24(1) Å vs 2.163(3) Å) while the Ta−N bond lengths are similar (1.969(8) (E = S) vs 1.958(3) (E = O) Å). The Ta−OAr distances are greater in the alkoxide complex (1.905(2), 1.918(2) Å) than in the thiolate complex, which suggests that the Ta−OAr bonds have less multiple bond character when the O^{t}Bu ligand is present. This can be taken as an indication that the ^{t}BuO ligand is a better π donor to the vacant Ta d_π orbitals. Also in comparing the Ta−ER distances, the Ta−O^{t}Bu distance is estimated to be 15% shorter than a single bond, while for E = S, the Ta−S^{t}Bu distance is only 6% shorter. While these data may be used to support the view that ^{t}BuO is a better π donor than ^{t}BuS, the differences in the Ta−C bond distances could be used to argue that overall the thiolate is a better ($\sigma + \pi$) donor.

This brings us to the crux of the matter. While it is generally accepted that element−element π bonding is favored for the lighter first-row elements because of their He core and small radius, the second-row elements are less electronegative and their 3s and 3p orbitals lie closer in energy to those of transition metals. [Compare the ionization energies of O and S: O 2p, 16 eV, vs S 3p, 12 eV, and O 2s, 32 eV, vs S 3s, 21 eV.][9] Which then is the better π donor—oxygen because of its small core or sulfur because its 3p orbitals are closer in energy to the metal d_π orbitals?

With these thoughts in mind, we set out to interrogate the difference between O^{t}Bu and S^{t}Bu ligands at $(M{=}M)^{6+}$ centers (M = Mo, W). We report herein our findings based on synthesis, structural, and spectroscopic studies together with insights gleened through the use of DFT B3LYP computations on model compounds.

Results and Discussion

Syntheses and Reactivity Studies of $M_2(O^tBu)_2(S^tBu)_4$ Compounds. Hydrocarbon solutions of $M_2(O^tBu)_6$ (M = Mo, W) react at room temperature with an excess of ^{t}BuSH to give the compounds $M_2(O^tBu)_2(S^tBu)_4$ which may be isolated as red air-sensitive and thermally sensitive, crystalline samples by crystallization from hexanes. In the case of molybdenum, the reaction is complete after 2 days and upon removal of solvent $Mo_2(O^tBu)_2(S^tBu)_4$ is obtained. However, some thermal decomposition occurs to give contamination with a black insoluble product. This is best removed by filtration and the desired mixed alkoxide thiolate is obtained by recrystallization of the hexane extract. In the case of tungsten, the substitution reaction proceeds more slowly and upon removal of the solvent after 2 days the crude product is composed of a mixture of $W_2(O^tBu)_2(S^tBu)_4$ (ca. 85%) and $W_2(O^tBu)_3(S^tBu)_3$ (ca. 15%). This crude mixture is then redissolved in benzene and a further excess of ^{t}BuSH is added and after stirring for 2 days the solvent and excess ^{t}BuSH and ^{t}BuOH are removed under a dynamic vacuum. Recrystallization from hexanes gives $W(O^tBu)_2(S^tBu)_4$ in close to 90% yield. This compound is less thermally sensitive than its molybdenum analogue though the progressive replacement of W−O^{t}Bu bonds is slower.

These reactions have been followed by ^{1}H NMR spectroscopy wherein $M_2(O^tBu)_6$ in benzene-d_6 or toluene-d_8 were allowed to react with an excess of ^{t}BuSH, ca. 10−20 equiv, at 22 °C. The concentrations of the compounds $M_2(O^tBu)_{6-n}(S^tBu)_n$, where $n = 1-4$, can be followed with time. A plot of the relative concentrations of the species detected by ^{1}H NMR spectroscopy for a reaction involving $W_2(O^tBu)_6$ for the first 800 min is given in Figure 1. After 2 days for M = Mo and ca. 5 days M = W, at 22 °C, the only species present in solution that are detectable by ^{1}H NMR spectroscopy are $M_2(O^tBu)_6$, $M_2(O^tBu)_2(S^tBu)_4$, ^{t}BuSH and the liberated ^{t}BuOH, thereby establishing the equilibrium shown in eq 4. The species $M_2(O^tBu)_{6-n}(S^tBu)_n$, where $n = 1, 2, 3$, are thus seen to be thermodynamically less stable than $M_2(O^tBu)_6$ and $M_2(O^tBu)_2(S^tBu)_4$.

$$M_2(O^tBu)_6 + 4^tBuSH \rightleftharpoons M_2(O^tBu)_2(S^tBu)_2 + 4^tBuOH \quad (4)$$

(4) McMillan, D. F.; Golden, D. G. *Annu. Rev. Phys. Chem.* **1982**, *33*, 493.

(5) Li, H.-C.; Nolan, S. P.; Peterson, J. L. *Organometallics* **1998**, *17*, 3516.

(6) For X = S see ref 5. For E = O see: Hartwig, J. F.; Andersen, R. A.; Bergman, R. G. *Organometallics* **1991**, *10*, 1875.

(7) Milstein, D.; Calabrese, J. C.; Williams, I. D. *J. Am. Chem. Soc.* **1986**, *108*, 6387.

(8) Fox, P. A.; Bruck, M. A.; Gray, S. D.; Gruhn, N. E.; Grittini, C.; Wigley, D. E. *Organometallics* **1998**, *17*, 2720.

(9) DeKock, R. L.; Gray, H B. In *Chemical Structure and Bonding*; University Science Books: Mill Hill, CA, 1989; see Table 4.4, p 227.

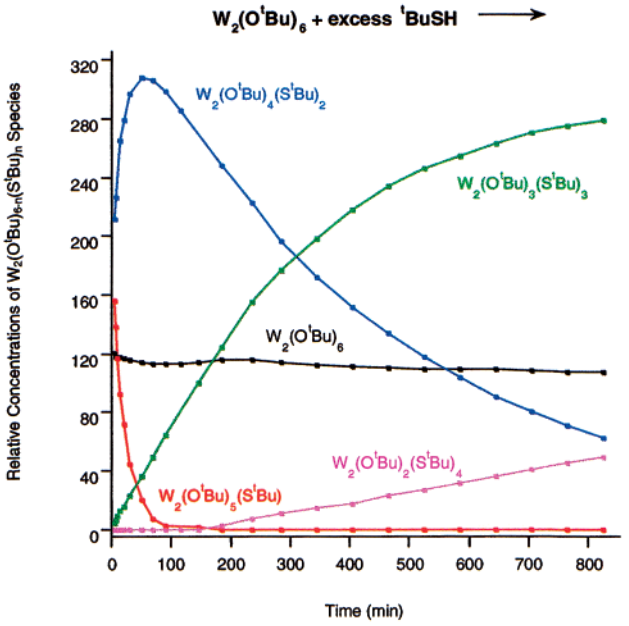

Figure 1. Relative concentrations of $W_2(O^tBu)_{6-n}(S^tBu)_n$, where $n = 0-4$, with time $t = 0-800$ min.

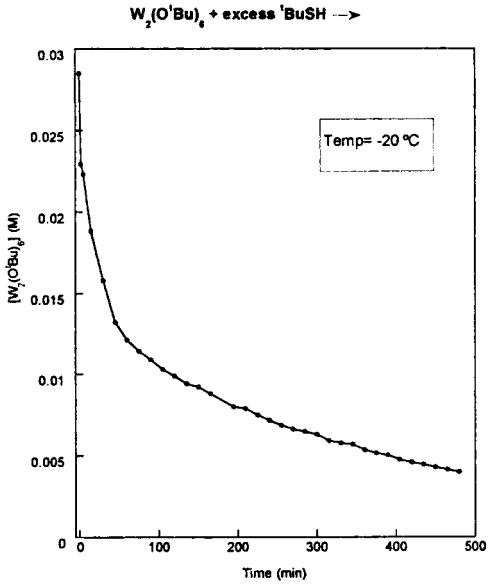

Figure 2. Concentration of $[W_2(O^tBu)_6]$ at −20 °C upon reaction with 20 equiv of ^{t}BuSH with time.

The initial reaction between $M_2(O^tBu)_6$ compounds and ^{t}BuSH is very fast and it is interesting to note that the concentrations of $M_2(O^tBu)_6$, excess ^{t}BuSH and liberated ^{t}BuOH change very little after 30 min at 22 °C. Upon cooling a toluene solution of $W_2(O^tBu)_6$ to −20 °C and following the reaction with 20 equiv of ^{t}BuSH one sees an approximate exponential loss in the concentration of $W_2(O^tBu)_6$ over a period of 500 min and an equilibrium is essentially attained after 1000 min. See Figure 2.

Addition of ^{t}BuOH to benzene-d_6 solutions of $M_2(O^tBu)_2(S^tBu)_4$ regenerates $M_2(O^tBu)_6$ compounds by way of the $M_2(O^tBu)_{6-n}(S^tBu)_n$ species, where $n = 3, 2, 1$. The ^{1}H NMR spectra reveal that the substitution pattern favors the stepwise substitution at each metal center and that rotation about the central M−M triple bond is rapid on the NMR time scale. Only in the case of M = Mo for the compound of formula $Mo_2(O^tBu)_4(S^tBu)_2$ did we see evidence of some consecutive substitution at the same metal center but even here the 1,1-$Mo_2(O^tBu)_4(S^tBu)_2$ isomer was present in a much smaller amount than its 1,2-isomer. No evidence for $(^tBuO)_3M{\equiv}M(S^tBu)_3$ was seen. The ^{t}BuO and ^{t}BuS signals come at significantly different chemical shift ranges (see the Experimental Section) so one can be certain in the assignment of signals arising for the $M_2(O^tBu)_{6-n}(S^tBu)_n$ species.

Though it has not proved possible to model the kinetics of the alkoxide/thiolate exchange, we have been able to estimate the values of K_{eq} for eq 4 over a limited temperature range by using ^{1}H NMR spectroscopy. For M = W, the equilibrium constant was found to be 0.016 at −1 °C and 0.0019 at 16 °C, while for M = Mo it was found to be 0.057 at −1 °C, 0.00099 at 16 °C and 0.000045 at 26 °C. Even these studies were hampered by the relative thermal instability of the compounds in solution. [Upon cooling below 22 °C the long time required for reactions to attain equilibrium becomes a complicating factor.] Nevertheless, we can estimate for M = Mo that for eq 4 $\Delta H° = -42(4)$ kcal mol^{-1} and $\Delta S° = -160(10)$ cal mol^{-1} K^{-1}. The rather large negative value of $\Delta S°$ is certainly noteworthy and presumably arises from hydrogen bonding factors in the solvent toluene-d_8. There is no evidence for inner-sphere coordination of ^{t}BuOH or ^{t}BuSH to the M_2 complexes by ^{1}H NMR spectroscopy though weak outer sphere complexation is likely,[10] as is the presence of $[^tBuOH]_x$ and $[^tBuOH]_y[^tBuSH]_z$ species in the solvent toluene-d_8. Given that the OH and SH bond dissociation energies are 105 and 92 kcal mol^{-1}, respectively for ^{t}BuOH and ^{t}BuSH,[11] we would expect that $\Delta H°$ = −52 kcal mol^{-1}. The enthalpy difference of 10 kcal mol^{-1} can thus be attributed, at least for the most part, to the difference in the average M−O and M−S bond strengths with the former being favored. This is significant, especially when compared to the enthalpy considerations noted earlier for the metals nickel and ruthenium (eqs 2 and 3) for which M−S was favored over M−O by 12 and 24 kcal mol^{-1}, respectively.[5] In conclusion, these equilibria studies reveal that the M−O^{t}Bu bonds are thermodynamically favored relative to their thiolate counterparts and even an excess of thiol fails to drive the equilibrium to $M_2(S^tBu)_6$.

Reactivity of $M_2(O^tBu)_2(S^tBu)_4$ toward Unsaturated Small Molecules. Unlike $M_2(O^tBu)_6$ compounds,[12] hydrocarbon solutions of $M_2(O^tBu)_2(S^tBu)_4$ show no reactivity toward CO (1 equiv), CO_2 (6 equiv), ethyne, ^{t}BuC≡CH, MeC≡N, and PhC≡N. This lack of reactivity is quite striking, although $M_2(SAr'')_6$ compounds, where Ar″ is 2,4,6-$Me_3C_6H_2$, were found to be similarly unreactive. The new compounds do, however, react with O_2 and NO. The detailed nature of the latter reactions have not been studied but it is evident from the preliminary studies of the reactions involving NO that ligand exchange (RO/SR) reactions complicate the formation and isolation of single products.

In another attempt to evaluate the relative influence of ^{t}BuS versus ^{t}BuO ligands, the reaction between $W_2(O^tBu)_6(\mu\text{-CO})$[13] and ^{t}BuSH was examined. As ^{t}BuS for ^{t}BuO exchange occurred the CO ligand was released. This was immediately apparent from ^{13}CO NMR studies employing the ^{13}CO labeled compound. By ^{1}H NMR spectroscopy one could see the formation of the $W_2(O^tBu)_{6-n}(S^tBu)_n$ compounds described previously. It was, however, possible to prepare nitrosyl complexes supported by

(10) Alaimo, P. J.; Bergman, R. G. *Organometallics* **1999**, *18*, 2707.
(11) Benson, S. W. *Chem. Rev.* **1978**, *78*, 23.
(12) Chisholm, M. H. *J. Chem. Soc., Dalton Trans.* **1996**, 1781.
(13) Chisholm, M. H.; Hoffman, D. M.; Huffman, J. C. *Organometallics* **1985**, *4*, 986.

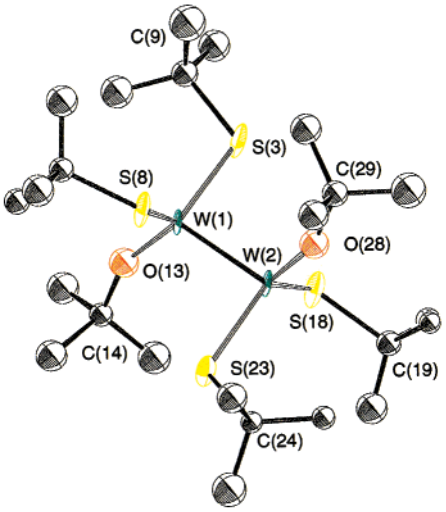

Figure 3. An ORTEP drawing of the molecular structure of $W_2(O^tBu)_2(S^tBu)_4$ showing the atom numbers used in Table 1. Thermal ellipsoids are drawn at the 50% probability level.

^{t}BuS ligands, which were analogues of previously characterized ^{t}BuO compounds, by the procedures outlined below.

$[Mo(StBu)_3(NO)]_2$ and $W(S^tBu)_3(NO)(py)$. Hydrocarbon solutions of $[Mo(O^tBu)_3(NO)]_2$14 and $W(O^tBu)_3(NO)(py)$[15] react with an excess of ^{t}BuSH to give complete replacement of the alkoxide ligands and formation of $[Mo(S^tBu)_3(NO)]_2$ and $W(S^tBu)_3(NO)(py)$, respectively. Both compounds are yellow and air-sensitive and were crystallized from toluene.

Single Crystal and Molecular Structures. $W_2(O^tBu)_2(S^tBu)_4$. The six E^{t}Bu ligands pack such that the central W_2 moiety is disordered over two possible sites within a pseudo O_2S_4 octahedron. This type of disorder is common for M_2X_8 and M_2X_6 complexes[16] and was seen, for example, in the structure of $W_2(OSiMe_2tBu)_6$, in which all three possible W_2 orientations were observed.[17] In the present case, only two sites were occupied and the disorder was modeled with occupancy factors of 0.93 and 0.07. The disorder is thus more of a nuisance than a problem with respect to the determination of molecular structure. While there is no doubt about the detailed nature of the coordination geometry, the structural parameters are not as precisely determined as one would like.

An ORTEP drawing of the molecule is given in Figure 3 and selected bond distances and bond angles are reported in Table 1. There is an anti ethane-like OS_2WWS_2O core with a W≡W distance of 2.333(4) Å. The W−W axis is collinear with the W−E−C planes, a structural situation that maximizes E p to W d π bonding. The W−O distances, 1.81(3) Å (av) and W−S distances, 2.31−2.36 Å, are fairly well determined and may be stated to be shorter than expected for pure single bonds as estimated from the sum of the covalent radii of W(3+) and O and S.[18] The effective shortening is ca. 0.2 Å for E = O and 0.1 Å for E = S which may be taken to imply a greater degree of oxygen to tungsten π bonding. The W−O−C angles of 155°

Table 1. Selected Bond Distances (Å) and Angles (deg) for the Major Isomer $W_2(O^tBu)_2(S^tBu)_4$

W(1)−W(2)	2.333(4)	W(1)−S(3)	2.32(1)
W(1)−S(8)	2.31(1)	W(1)−O(13)	1.81(3)
W(2)−S(18)	2.30(1)	W(2)−S(23)	2.31(1)
W(2)−O(28)	1.81(3)	S(3)−C(4)	1.84(4)
S(8)−C(9)	1.87(3)	S(18)−C(19)	1.91(3)
S(23)−C(24)	1.88(4)	O(13)−C(14)	1.40(4)
O(28)−C(29)	1.45(4)		
W(2)−W(1)−S(3)	94.8(2)	W(2)−W(1)−S(8)	93.4(3)
W(2)−W(1)−O(13)	114.0(8)	S(3)−W(1)−S(8)	118.9(4)
S(3)−W(1)−O(13)	114.0(8)	S(8)−W(1)−O(13)	117.1(8)
W(1)−W(2)−S(18)	97.1(3)	W(1)−W(2)−S(23)	94.2(2)
W(1)−W(2)−O(28)	112.1(8)	S(18)−W(2)−S(23)	116.9(4)
S(18)−W(2)−O(28)	115.9(8)	S(23)−W(2)−O(28)	116.2(8)
W(1)−S(3)−C(4)	109(1)	W(1)−S(8)−C(9)	113(1)
W(2)−S(18)−C(19)	110(1)	W(2)−S(23)−C(24)	111(1)
W(1)−O(13)−C(14)	155(2)	W(2)−O(28)−C(29)	158(2)

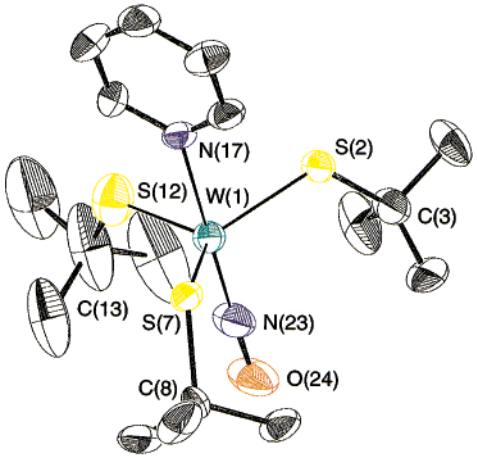

Figure 4. An ORTEP drawing of the molecular structure of $W(S^tBu)_3(NO)(py)$ showing the atom numbers used in Table 2. Thermal ellipsoids are drawn at the 50% probability level.

Table 2. Selected Bond Distances (Å) and Angles (deg) for $W(S^tBu)_3(NO)(py)$

W(1)−N(23)	1.773(7)	W(1)−S(12)	2.193(3)
W(1)−N(17)	2.291(7)	W(1)−S(2)	2.293(2)
W(1)−S(7)	2.317(2)	S(2)−C(3)	1.835(9)
S(7)−C(8)	1.860(8)	S(12)−C(13)	1.68(2)
N(23)−O(24)	1.197(9)		
N(23)−W(1)−S(12)	98.0(3)	N(23)−W(1)−N(17	175.5(4)
S(12)−W(1)−N(17)	85.5(2)	N(23)−W(1)−S(2)	99.6(3)
S(12)−W(1)−S(2)	113.6(1)	N(17)−W(1)−S(2)	81.4(2)
N(23)−W(1)−S(7)	98.1(3)	S(12)−W(1)−S(7)	120.10(9)
N(17)−W(1)−S(7)	77.7(2)	S(2)−W(1)−S(7)	119.82(8)
C(3)−S(2)−W(1)	116.9(3)	C(8)−S(7)−W(1)	116.2(3)
C(13)−S(12)−W(1)	120.2(7)	C(18)−N(17)−W(1)	120.4(5)
C(22)−N(17)−W(1)	122.8(6)	O(24)−N(23)−W(1)	177.0(9)

and 158° are also notably larger than the W−S−C angles which fall within a narrow range of 111(±2)°. The significance of these angles on ligand pπ to metal dπ bonding will be discussed later.

$W(S^tBu)_3(NO)(py)$. An ORTEP drawing of the molecule is given in Figure 4 and selected bond distances and bond angles are listed in Table 2. This trigonal bipyramidal molecule bears a very close resemblance to its ^{t}BuO analogue[15] and a comparison of selected structural parameters is given in Table 3. The W−N distance appears shorter and the N−O distance longer in the ^{t}BuO derivative relative to the thiolate but, within the limit of 3σ, they may be stated to be indistinguishable. Again

(14) Chisholm, M. H.; Cotton, F. A.; Extine, M. W.; Kelly, R. L. *J. Am. Chem. Soc.* **1978**, *100*, 3354.
(15) Chisholm, M. H.; Cotton, F. A.; Extine, M. W.; Kelly, R. L. *Inorg. Chem.* **1979**, *18*, 116.
(16) Cotton, F. A.; Walton, R. A. *Multiple Bonds Between Metal Atoms*, 2nd ed.; Oxford University Press: Oxford, U.K., 1994.
(17) Chisholm, M. H.; Cook, C.; Huffman, J. C.; Streib, W. E. *J. Chem. Soc., Dalton Trans.* **1991**, 929.
(18) Chisholm, M. H.; Corning, J. F.; Huffman, J. C. *Inorg. Chem.* **1984**, *23*, 754.

Table 3. Comparison of Selected Structural Parameters for the Related Molecules W(E^{t}Bu)$_3$(NO)(py), Where E = O and

	E = O	E = S		E = O	E = S
W−E (av) (Å)	1.89(1)	2.268(4)	W−E−C (deg)	135(1)	117.8(8)
W−N (NO) (Å)	1.732(8)	1.773(7)	W−N−O (deg)	179.2(8)	177.0(9)
W−N (py) (Å)	2.323(7)	2.291(7)	E−W−N (NO) (deg)	100.3(5)	98.6(5)
N−O (Å)	1.25(1)	1.197(9)			

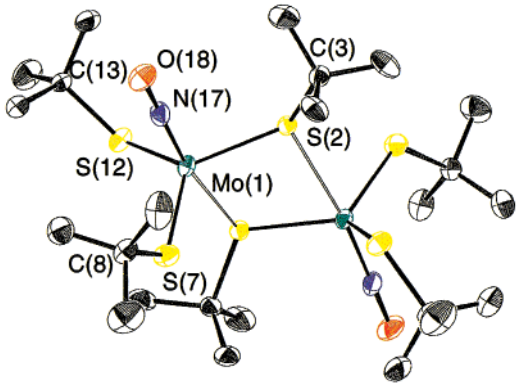

Figure 5. An ORTEP drawing of the molecular structure of [Mo(S^{t}Bu)$_3$NO]$_2$ showing the atom numbers used in Table 4. Thermal ellipsoids are drawn at the 50% probability level.

Table 4. Selected Bond Distances (Å) and Bond Angles (deg) for [Mo(S^{t}Bu)$_3$NO]$_2$

Mo(1)−S(2)	2.384(3)	Mo(1)−S(2)	2.610(3)
Mo(1)−S(7)	2.289(3)	Mo(1)−S(12)	2.293(3)
Mo(1)−N(17)	1.768(7)	S(2)−C(3)	1.876(9)
S(7)−C(8)	1.876(9)	S(12)−C(13)	1.842(9)
O(18)−N(17)	1.217(8)		
S(2)−Mo(1)−S(2)	74.06(9)	S(2)−Mo(1)−S(7)	122.40(9)
S(2)−Mo(1)−S(7)	88.88(8)	S(2)−Mo(1)−S(12)	114.87(9)
S(2)−Mo(1)−S(12)	83.50(8)	S(2)−Mo(1)−N(17)	97.2(2)
S(2)−Mo(1)−N(17)	170.9(2)	S(7)−Mo(1)−S(12)	117.2(1)
S(7)−Mo(1)−N(17)	98.3(3)	S(12)−Mo(1)−N(17)	98.1(3)
Mo(1)−S(2)−Mo(1)	100.71(8)	Mo(1)−S(2)−C(3)	119.6(3)
Mo(1)−S(2)−C(3)	124.0(3)	Mo(1)−S(7)−C(8)	118.8(3)
Mo(1)−S(12)−C(13)	118.3(3)	Mo(1)−N(17)−O(18)	178.7(7)

the W−O−C angles are notably larger than the W−S−C angles which fall within the range 116 to 120°.

[Mo(S^{t}Bu)$_3$(NO)]$_2$. An ORTEP drawing of this molecule is given in Figure 5. The geometry about each molybdenum is a distorted trigonal bipyramid. The two halves of the molecule are united by a pair of thiolate bridging groups which occupy equatorial and axial sites. The axial Mo−S bonds are longer, 2.610(3) versus 2.384(3) Å, and are trans to the linear M−N−O moiety. Selected structural parameters are given in Table 4. This structure bears a close relationship with its ^{t}BuO analogue[14] though the longer Mo−S bonds lead to an even greater nonbonded separation of Mo atoms, 3.85 versus 3.33 Å. A comparison of selected structural parameters is shown in Table 5. Once again the structural parameters associated with the Mo−N−O moiety are statistically equivalent.

Spectroscopic Characterization. The ^{1}H NMR spectra of the M$_2$(O^{t}Bu)$_{6-n}$(S^{t}Bu)$_n$ compounds are reported in the Experimental and as noted earlier support the ethane-like nature of this class of compounds wherein rotation about the M≡M bond is rapid on the NMR time-scale. The substitution pattern about the M$_2$ center is readily determined by the integral ratios of the ^{t}Bu signals. For [Mo(S^{t}Bu)$_3$(NO)]$_2$ there are two ^{t}BuS singlets in the ratio of 2:1 in the temperature range −80 to +80 °C in toluene-d_8. This is consistent with expectations based on the solid-state structure and shows that the bridge ⇄ terminal group exchange is slow relative to that seen for the ^{t}BuO analogue. For W(S^{t}Bu)$_3$(NO)(py) the ^{1}H NMR spectra are simple as expected for a monomer.

In the infrared spectra the most significant features are the appearance of υ(NO) for the linear M−N−O moieties. For W(S^{t}Bu)$_3$(NO)(py) and [Mo(S^{t}Bu)$_3$NO]$_2$ the NO stretching frequencies appear at higher wavenumber than their ^{t}BuO analogues. As we have noted[14,15] before, this value of υ(NO) is greatly influenced by both the metal and the ancillary (spectator) ligands in compounds of the formula MX$_3$(NO), where M = a group 6 metal (Cr, Mo, W) and representative examples are given in Table 6. The lower the value of υ(NO) in a related series of compounds the greater the degree of metal d_π to NO π^* back-bonding. The problem of separating σ and π effects will be described later. For the group 6 metals shown in Table 6, this involves formally the $(d_{xz}, d_{yz})^4$ metal orbitals if the M−N−O axis is classified as the z axis and the oxidation state of the metal assigned to be +2 as a result of counting a linear metal nitrosyl as M− ← (NO$^+$), an electron counting scheme that emphasizes the isolobal relationship of NO$^+$ and CO in their bonding to a metal center.

To probe the influence of the ^{t}BuO and ^{t}BuS ligands on the electronic structure and bonding in these closely related compounds, we resorted to computational methods applied to model compounds as outlined below.

Electronic Structure Calculations. Density functional calculations have been performed on the M$_2$(EH)$_6$ M$_2$(OH)$_2$(SH)$_4$, W(EH)$_3$(NO)(NH$_3$) and (HE)$_3$MCMe molecules and the M(EH)$_3$ and CMe fragments, where M = Mo, W and E = O, S, to gain insight in the differences between oxygen and sulfur ligation. Orbital energy diagrams, Mulliken charge distributions and bond energies were compared to address this issue.

As a starting point, B3LYP[19] calculations with the LANL2DZ[20] basis were done using the Gaussian 98 program.[21] Due to relatively small differences in the bond energies calculated and to give a better approximation to experimental data, better basis sets were then applied. A triple-zeta basis set (CEP-121G)[22] with polarization functions added for oxygen and sulfur was used to give more accurate results. This basis set was used in combination with both the CEP and LANL2 effective core potentials.

(19) Becke, A. D. *J. Chem. Phys.* **1993**, *98*, 5648.

(20) (a) Hay, P. J.; Wadt, W. R. *J. Chem. Phys.* **1985,** *82*, 270. (b) Wadt, W. R.; Hay, P. J. *J. Chem. Phys.* **1985**, *82*, 284. (c) Hay, P. J.; Wadt, W. R. *J. Chem. Phys.* **1985,** *82*, 299.

(21) Frisch, M. J.; Trucks, G. W.; Schlegel, H. B.; Scuseria, G. E.; Robb, M. A.; Cheeseman, J. R.; Zakrzewski, V. G.; Montgomery, Jr., J. A.; Stratmann, R. E.; Burant, J. C.; Dapprich, S.; Millam, J. M.; Daniels, A. D.; Kudin, K. N.; Strain, M. C.; Farkas, O.; Tomasi, J.; Barone, V.; Cossi, M.; Cammi, R.; Mennucci, B.; Pomelli, C.; Adamo, C.; Clifford, S.; Ochterski, J.; Petersson, G. A.; Ayala, P. Y.; Cui, Q.; Morokuma, K.; Malick, D. K.; Rabuck, A. D.; Raghavachari, K.; Foresman, J. B.; Cioslowski, J.; Ortiz, J. V.; Stefanov, B. B.; Liu, G.; Liashenko, A.; Piskorz, P.; Komaromi, I.; Gomperts, R.; Martin, R. L.; Fox, D. J.; Keith, T.; Al-Laham, M. A.; Peng, C. Y.; Nanayakkara, A.; Gonzalez, C.; Challacombe, M.; Gill, P. M. W.; Johnson, B.; Chen, W.; Wong, M. W.; Andres, J. L.; Gonzalez, C.; Head-Gordon, M.; Replogle, E. S.; Pople, J. A. *Gaussian 98*, Revision A.6; Gaussian, Inc.: Pittsburgh, PA, 1998.

(22) (a) Stevens, W. J.; Basch, H.; Krauss, M. *J. Chem. Phys.* **1984**, *81*, 6026. (b) Stevens, W. J.; Basch, H.; Krauss, M.; Jasien, P. G. *Can. J. Chem.* **1992**, *70*, 612. (c) Cundari, T. R.; Stevens, W. J. *J. Chem. Phys.* **1993**, *98*, 5555.

Table 5. Comparison of Selected Bond Distances (Å) and Angles (deg) for the Related Compounds $[Mo(E^tBu)_3NO]_2$, Where E=O, S

	E = O	E = S		E = O	E = S
Mo···Mo	3.334(2)	3.85	M−N−O	178(1)	178.7(7)
Mo−E (μ, eq)	1.951(6)	2.384(3)	N−M−E (av)	99.7(7)	97.9(4)
Mo−E (μ, axial)	2.195(6)	2.610(3)	M−E−M	106.9(3)	100.71(8)
Mo−E (terminal, eq)	1.850(7)	2.289(3)	M−E−C	125(1)	118.9(5)
Mo−E (terminal, eq)	1.861(6)	2.293(3)			
Mo−N (NO)	1.747(9)	1.768(7)			
N−O	1.21(1)	1.217(8)			

Table 6. Values of ν(NO) for Various $MX_3(NO)$ Compounds, Where M = Cr, Mo, and W and X = Amide, Alkoxide, Siloxide, and Thiolate

compound	ν(NO) (cm^{-1})	ref	compound	ν(NO) (cm^{-1})	ref
$W(O^tBu)_3(NO)(py)$	1555	15	$Mo(NO)(OSiMe_2{}^tBu)_3(py)_2$	1624	c
$[Mo(OCH2tBu)_3NO]_2$	1643	14	$W(NO)(OSiMe_2{}^tBu)_3(py)_2$	1542	c
$[Mo(O^iPr)_3NO]_2$	1640	14	$Mo(SC_6H_2{}^iPr_3\text{-}2,4,6)_3(NO)(NH_3)$	1680	c
$[Mo(O^tBu)_3NO]_2$	1632	14	$[Mo(SAd)_3NO]_2$	1642	d
$[Mo(OSiMe_2{}^tBu)_3NO]_2$	1648	a	$W(S^tBu)_3(NO)(py)$	1604	e
$Cr(N(SiMe_3)_2)_3NO$	1698	b	$[Mo(S^tBu)_3NO]_2$	1644	e
$Cr(N^iPr_2)_3NO$	1640	b			

[a] Chisholm, M. H.; Cook, C. M.; Folting, K.; Streib, W. E. *Inorg. Chim. Acta* **1992**, *198−200*, 63. [b] Bradley, D. C.; Hursthouse, M. B.; Newing, C. W.; Welch, A. J. *J. Chem. Soc., Chem. Comm.* **1972**, 567. [c] Bishop, P. T.; Dilworth, J. R.; Hutchinson, J.; Zubieta, J. *J. Chem. Soc., Dalton Trans.* **1986**, 967. [d] Agapie, T.; Odom, A. L.; Cummins, C. C. *Inorg. Chem.* **2000**, *39*, 174. [e] This work.

In addition, density functional calculations were performed using ADF 2000.02.[23] For these calculations, a triple-zeta basis set was chosen with polarization functions for oxygen, sulfur and hydrogen. BLYP[24] with ZORA[25] relativistic terms was used.

It is important to note that all of the above calculations show similar trends. A comparison of the different computational results will be given in the Supporting Information. For the sake of simplicity, only the calculations using CEP-121G with polarization functions added to O and S and the CEP effective core potential will be discussed in the text. The triple-zeta basis set is obviously superior to the double-zeta and the CEP effective potential was chosen because it retains the same number of electrons for O and S outside the core.

$M_2(EH)_6$ compounds. As a starting point the coordinates from the X-ray crystal structure of $Mo_2(OCH_2tBu)_6$[26] were chosen and the α-carbon atoms replaced by hydrogen atoms. The calculations then proceeded to calculate a minimum energy and optimum geometry. A similar approach was taken for the $M_2(SH)_6$ molecules (M = Mo, W) wherein H replaced the α-carbon of the mesityl group of $W_2(SAr'')_6$ where Ar″ is 2,4,6-$Me_3C_6H_2$.[27]

For $M_2(OH)_6$ the DFT B3LYP calculations closely parallel the earlier Xα calculations[16] in their prediction that the frontier orbitals are the M−M π and σ orbitals, though both have some mixing with M−O bonding. The HOMO's are degenerate M−M π-orbitals of e_u symmetry at −6.95 eV (M = Mo) and −6.32 eV (M = W). These orbitals have significant M−O π* character as a result of the M d_π-O p_π interactions as shown in Figure 6. The next lower energy orbitals are the σ orbitals having principally M−M bonding character (d_{z^2}-d_{z^2}) but there is some O p_π involvement and again this is M−O antibonding as is shown in Figure 7. For both M = Mo and W respectively, the highest energy σ orbital is calculated to be at −7.65 and −7.79 eV. These values find close agreement with the observed photoelectron spectroscopic values for the 1st and 2nd ionization potentials of $M_2(O^tBu)_6$ compounds.[16]

In contrast, the HOMO of the $M_2(SH)_6$ molecules have no metal character but are sulfur out-of-phase lone-pair combinations as shown in Figure 8. These occur at essentially the same energy for both metals, with the HOMO at −7.14 eV for W and −7.12 eV for Mo. The M−M π-bonding orbitals are found at considerably lower energies, namely −7.77 eV (M = Mo) and −7.36 eV (M = W).

A comparison of the orbital energies of the $M_2(SH)_6$ molecules is shown in Figure 9 and a comparison of the orbital energies of $W_2(OH)_6$ and $W_2(SH)_6$ is given in Figure 10. It is thereby apparent that the $M_2(SH)_6$ molecules have very similar electronic structures although there is a switching of the relative stabilities of the e_u and a_{1u} orbitals (M−M π + M−S π* vs. S in-phase lone-pair combination), as well as the lower energy e_u and a_{2u}. In contrast, as is shown in Figure 10, the influence of O pπ to M d_π bonding results in a greatly different spread of the orbitals of E symmetry, cf. 4.3 eV for E = O vs 1.7 eV for E = S. These orbitals are M−M π in character with a M−E π* contribution for the destabilized orbitals and with a M−E π contribution for the stabilized orbital. Thus the spread of the orbitals is a clear indication of the greater importance of the M−O π interactions. The frontier orbitals of the $M_2(OH)_6$ molecules which may be classified as M−M π and σ are greatly raised (destabilized) in energy as a result of O p_π to M d_π antibonding. The calculated structural parameters for the $M_2(EH)_6$ molecules are given in Table 7.

An inspection of the Mulliken charge distributions is also interesting. For $M_2(OH)_6$ there is significant bond polarity with each metal carrying a formal +1.1 unit of charge and each oxygen a −0.8 charge. In contrast, $M_2(SH)_6$ molecules have essentially covalent M−S bonds and no significant charge resides on either M or S. The calculations support the view that the M-OH bonds are notably more ionic than the M-SH bonds,

(23) (a) ADF2000.02. (b) Baerends, E. J.; Ellis, D. E.; Ros, P. *Chem. Phys*. **1973,** *2*, 41. (c) Versluis, L.; Ziegler, T. *J. Chem. Phys* **1988**, *322*, 88. (d) te Velde, G.; Baerends, E. J. *J Comput. Phys* **1992,** *99* (1), 84. (e) Guerra, C. F.; Snijders, J. G.; te Velde, G.; Baerends, E. J. *Theor. Chem. Acc.* **1998**, *99*, 391.

(24) (a) Lee, C.; Yang, W.; Parr, R. G. Development of the Colle-Salvetti correlation-energy formula into a functional of the electron density. *Phys. Rev. B* **1988**, *37*, 785. (b) Miehlich, B.; Savin, A.; Stoll, H.; Preuss, H. *Chem. Phys. Lett.* **1989,** *157*, 200. (c) Becke, A. D. *Phys. Rev. A* **1988**, *38*, 3098.

(25) (a) Snijders, J. G.; Baerends, E. J.; Ros, P. *Mol. Phys.* **1979**, *38*, 1909. (b) Ziegler, T.; Tschinke, V.; Baerends, E. J.; Snijders, J. G.; Ravenek, W. *J. Phys. Chem.* **1989**, *93*, 3050. (c) van Lenthe, E.; Baerends, E. J.; Snijders, J. G. **1993**, *99*, 4597.

(26) Chisholm, M. H.; Cotton, F. A.; Murillo, C. A.; Reichert, W. W. *Inorg. Chem.* **1977**, *16*, 1801.

(27) Chisholm, M. H.; Corning, J. F.; Folting, K.; Huffman, J. C. *Polyhedron* **1985**, *4*, 383.

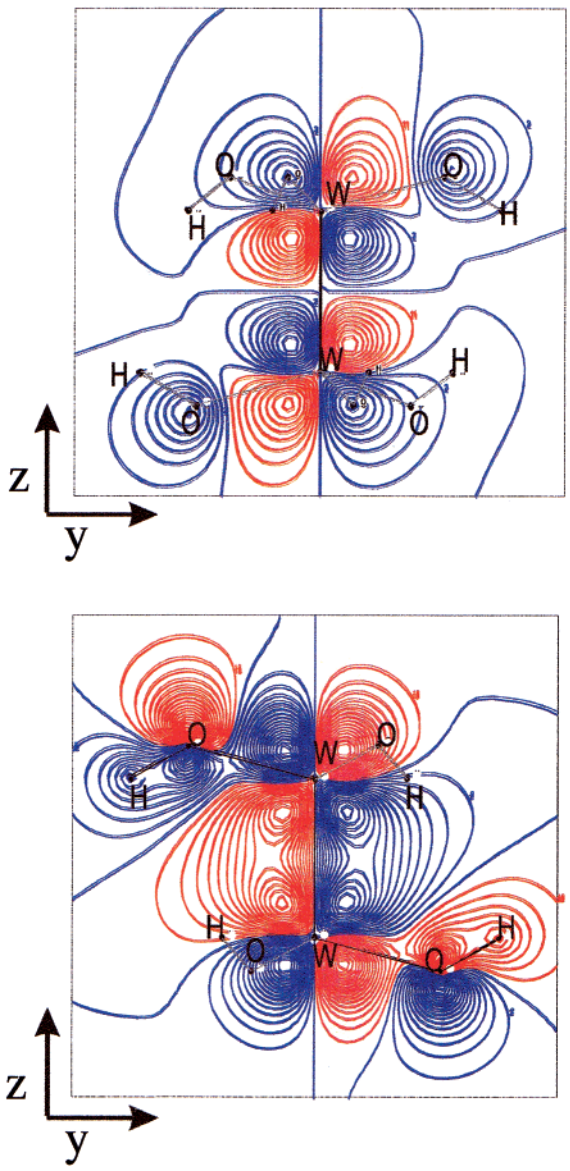

Figure 6. Contour plots of the LUMO (top) and HOMO (bottom) for the $W_2(OH)_6$ molecule showing the M−M π^* (LUMO) and π (HOMO) bonding character with M−O π^* character.

as would be expected based in the electronegativity of oxygen and sulfur.

Finally, it should be mentioned that the minimized energies of the $M_2(EH)_6$ molecules differed little for M−E-H moieties displaced either proximal or distal to the M−M triple bond. It is the D_{3d} structure that is favored in both cases as this maximizes M−M and M−E π bonding. The all proximal $M_2(OH)_6$ was slightly favored but, as is seen in the structures of various $M_2(OR)_6$ compounds[28] and the $W_2(O^tBu)_2(S^tBu)_4$ structure reported here, combinations of proximal and distal ligands may be found presumably as a result of steric factors.

$M_2(OH)_2(SH)_4$. Calculations were also performed on $M_2(OH)_2(SH)_4$ molecules having idealized C_{2h} symmetry. The bond lengths and angles are given in Table 7 and are consistent with the structural parameters for $W_2(O^tBu)_2(S^tBu)_4$; the W−O−H and W−W−O angles are greater than the W−S−H and W−W−S angles, respectively. Here the degeneracy of the e orbitals is removed and the HOMO is calculated to be a M−M π + M−O π^* molecular orbital at −6.92 eV and −7.33 eV for W and Mo, respectively. The HOMO is 0.6 eV for W and 0.4 eV for Mo lower in energy than that in the $M_2(OH)_6$ molecules and is closer in energy to the sulfur lone-pairs. The replacement of four OH groups by four SH groups leads to a stabilization of the HOMO and increased localized M−O π-bonding.

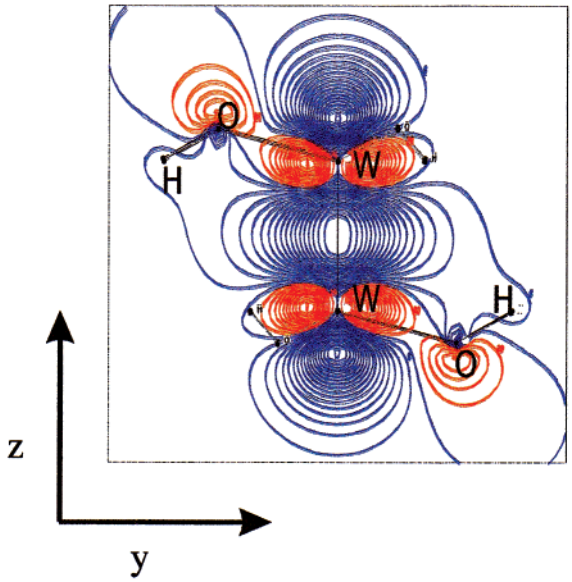

Figure 7. Contour plot of the M−M σ bonding orbital in $W_2(OH)_6$ showing the Wd_{z^2}–Wd_{z^2} and O p_π mixing.

$W(EH)_3(NO)(NH_3)$. Calculations were also performed on $W(EH)_3(NO)(NH_3)$ having C_{3v} symmetry as models for the compounds $W(E^tBu)_3(NO)(py)$, where E = O and S. In both cases the HOMO was a degenerate orbital of E symmetry being metal $(d_{xz}, d_{yz})^4$ with bonding to the N−O π^* molecular orbital. When E = O, the MO was higher in energy and there was greater N−O π^* occupation. See Table 8 and Figures11 and 12. An inspection of the Mulliken charges again revealed that the M−O bonds were more polar with W +1.18 and O −0.81 versus W +0.14 and S −0.19 in the respective OH and SH complexes.

$M(EH)_3$ Fragments. The separation of σ and π effects of ligands in transition metal chemistry is difficult. However, the classic case of the influence of π-bonding is in octahedral ML_6 complexes where Δ_o, the separation between the e_g (M−L dσ^* orbitals) and t_{2g} (the M d π orbitals), is increased by π-acceptor ligands and decreased by π-donor ligands. However, a very strong σ-donor ligand can still produce a large Δ_o value because the e_g orbitals have M−L σ^* character and the t_{2g} orbitals are nonbonding. For a planar ML_3 fragment the d orbital splitting pattern is $(d_{xy}, d_{x^2-y^2})$ above d_{z^2} which is in turn above (d_{xz}, d_{yz}). The latter have no possibility of interacting with the σ set of orbitals, while the $(d_{xy}, d_{x^2-y^2})$ and d_{z^2} (because of its taurus) do participate in M−L σ bonding. It was, therefore, pertinent to examine the bonding in the $(HE)_3M$ fragments to compare the influence of E = O versus S on the d orbital splitting pattern.

The calculations predicted that in all cases the fragments with three unpaired electrons were lower in energy than those with only one unpaired electron (see Supporting Information). An orbital energy level diagram of the $(HE)_3W$ fragment is given in Figure 13 and that for the molybdenum counterpart is given in Figure 14.

For $W(OH)_3$, the (d_{xz}, d_{yz}) orbitals lie higher in energy than the d_{z^2} orbital, compare −5.53 eV versus −6.48 eV. Below these lie the oxygen lone-pairs. The $W(SH)_3$ fragment also

(28) (a) Chisholm, M. H. *Polyhedron* **1983**, *2*, 681. (b) Chisholm, M. H.; Clark, D. L.; Folting, K.; Huffman, J. C.; Hampden-Smith, M. J. *J. Am. Chem. Soc.* **1987**, *109*, 7750. (c) Chisholm, M. H.; Folting, K.; Hampden-Smith, M. J.; Smith, C. A. *Polyhedron* **1987**, *6*, 1747.

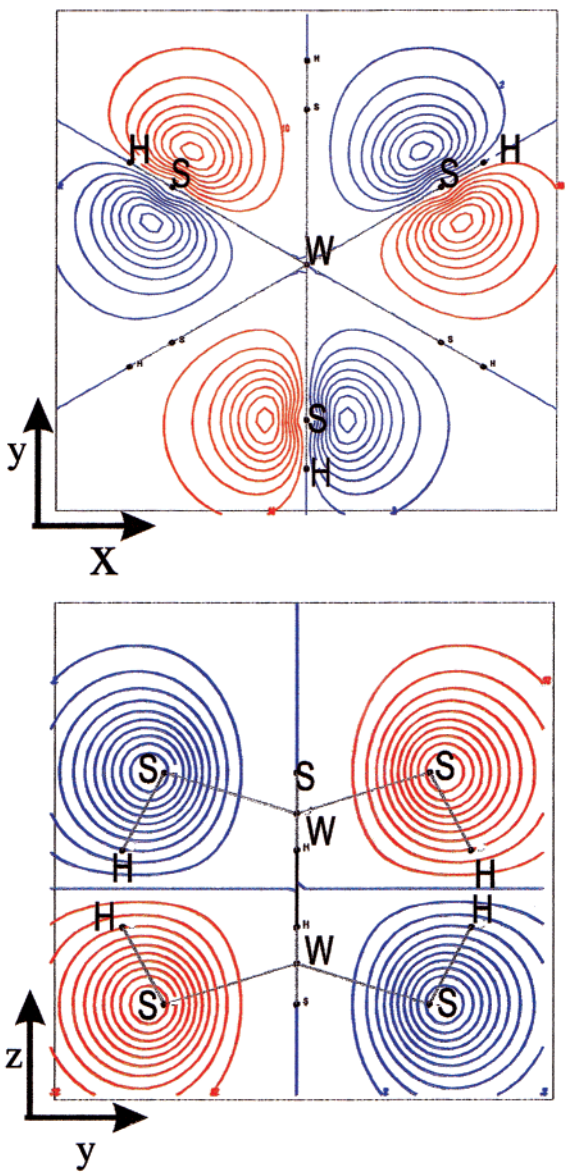

Figure 8. Contour plot of the HOMO of $W_2(SH)_6$ showing the sulfur lone pair character viewed down the M−M axis (top) and perpendicular to the M−M bond (bottom).

reveals the order (d_{xz}, d_{yz}) above d_{z^2}, but the energies are lower by ca. 0.5 eV and the energy difference between the e and a_1 orbitals is smaller. The sulfur lone-pairs are closer in energy to the metal based orbitals.

For the $Mo(OH)_3$ fragment the (d_{xz}, d_{yz}) orbitals again lie above the d_{z^2} but the separation in orbital energy is smaller, only 0.24 eV. For the $Mo(SH)_3$ fragment the HOMO is a sulfur lone-pair combination of A_2 symmetry in the C_{3V} point group. Below that comes the d_{z^2} orbital which is now higher in energy than the (d_{xz}, d_{yz}) degenerate orbitals of E symmetry.

Bearing in mind that strong σ donation can drive up the energy of the d_{z^2} orbital we see that for each $M(EH)_3$ fragment this is higher for E = O than for E = S. That the (d_{xz}, d_{yz}) is above the d_{z^2} is a sure indication of the importance of the E pπ to M dπ back-bonding. For W, the energy separation of nearly 1.0 eV for E = O versus 0.3 eV for E = S indicated that though S pπ to Wd π bonding is significant it is less than that for E = O. In the case of M = Mo, only when E = OH does the (d_{xz}, d_{yz}) orbital lie above the d_{z^2} orbital, again a clear indication of the greater O pπ to W dπ bonding. The greater π-influence of

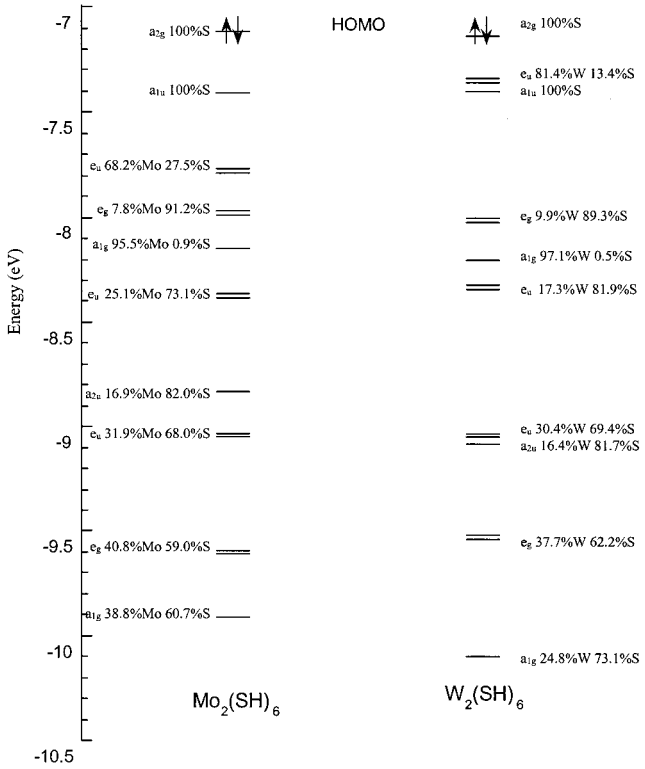

Figure 9. An orbital energy level diagram comparing the frontier molecular orbital energies of the $M_2(SH)_6$ molecules, where M = Mo, W, with Mulliken populations.

EH pπ orbitals on tungsten can be attributed to the greater radial extension of its 5d orbitals relative to Mo 4d orbitals. The absolute orbital energies also reflect the effective nuclear charge of the metal atoms and the great shielding exerted by the tungsten electrons.

Estimate of M≡M, M-EH and M≡CMe Bond Energies. Several estimates of the strength of the M=M bond in M_2X_6 compounds have been previously made based on experimental data obtained from calorimetric studies[29] and from calculations on model compounds.[30] The experimental data lead to problems of separation of M−X and M≡M bond energies with the former having to be estimated from mononuclear complexes with the metal atoms in different oxidation states. Computational methods lead to estimates which vary with method. A comparison of previous estimates of the M≡M bond strength in $M_2(OR)_6$ and the model compounds $M_2(OH)_6$ is presented in Table 9, along with the predictions for the $M_2(EH)_6$ compounds from this study. While the absolute numbers vary, they do so in a rather consistent manner. The Mo−Mo triple bond strength is roughly two-thirds of the W−W triple bond strength, a ratio which finds similarity to that of the M−M bond strength of the metals as determined by their heats of vaporization.[31] Our values of ca. 90 kcal/mol for $W_2(OH)_6$ are very similar to previous estimates, while the value obtained for $W_2(SH)_6$ is new. If our calculations are reliable, we predict that the W−W bond strength in $W_2(SR)_6$ compounds should be less than in the related $W_2(OR)_6$ compounds. The difference for related $Mo_2(ER)_6$ compounds appears to be less, but in the same order.

Why then does alkyne metathesis occur for $W_2(OR)_6$ compounds, but not for the related $W_2(SR)_6$ compounds? To address

(29) Connor, J. A.; Pilcher, G.; Skinner, H. A.; Chisholm, M. H.; Cotton, F. A. *J. Am. Chem. Soc.* **1978**, *100*, 7738.

(30) (a) Kok, R. A.; Hall, M. A. *Inorg. Chem.* **1983**, *22*, 728. (b) Ziegler, T.; Tschinke, V.; Becke, A., *Polyhedron* **1987**, *6*, 685.

(31) Greenwood, N. N.; Earnshaw, A. *Chemistry of the Elements*; Pergamon Press: New York, 1984.

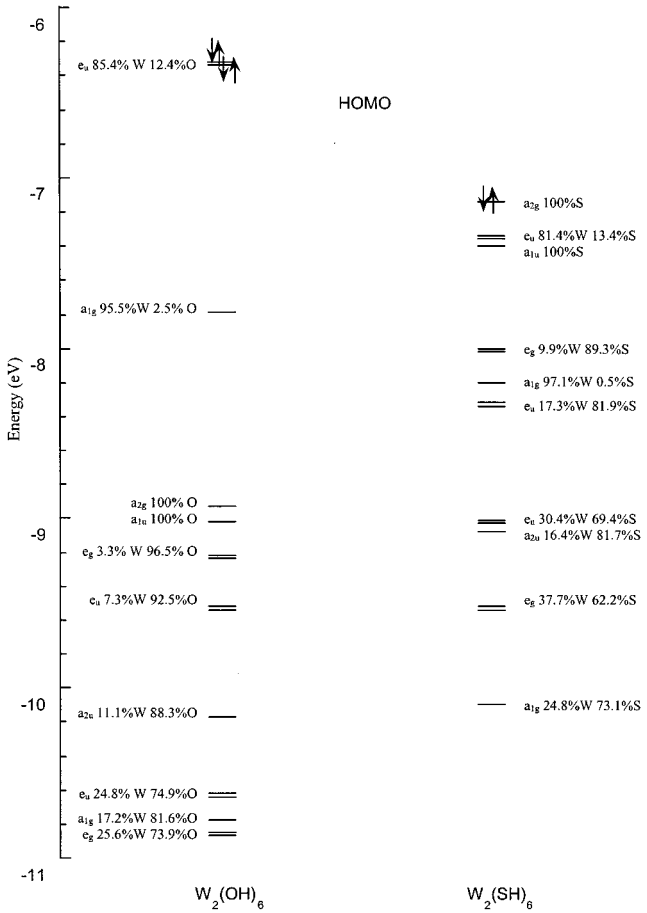

Figure 10. A comparison of the frontier molecular orbital energies for the $W_2(OH)_6$ and $W_2(SH)_6$ molecules with Mulliken populations.

Table 7. Calculated Optimized Structural Parameters for $W_2(OH)_2(SH)_4$ and the $M_2(EH)_6$ Molecules, Where M = Mo and W and E = O and S, Using Gaussian B3LYP CEP-121G with Polarization Added for O and S and the CEP Effective Core Potential

	M−M (Å)	M−E (Å)	E−H (Å)	M−M−E (deg)	M−E−H (deg)
$Mo_2(OH)_6$	2.258	1.924	0.970	103.7	123.9
$W_2(OH)_6$	2.317	1.915	0.969	104.8	124.1
$Mo_2(SH)_6$	2.226	2.355	1.359	105.3	103.8
$W_2(SH)_6$	2.285	2.354	1.359	105.1	104.2
$W_2(OH)_2(SH)_6$	2.297				
E = O		1.899	0.970	107.5	124.7
E = S		2.360	1.360	103.2	104.6

this question we have calculated the W≡CMe energies in the related $(EH)_3W{\equiv}CMe$ molecules. As is shown in Table 9, the W≡C bond strengths are on the order of 136 kcal/mol for E = O and 129 kcal/mol for E = S. By using the same computational procedure, we calculate the C≡C bond energy in MeC≡CMe to be 181 kcal/mol. Thus, for the reaction shown in eqn. **5**, we calculate the

$$(HE)_3M{\equiv}M(EH)_3 + MeC{\equiv}CMe \rightarrow 2[(HE)_3M{\equiv}CMe] \quad (5)$$

ΔH values listed in Table 9. A similar set of calculations performed for $Mo_2(EH)_6$ and MeC≡CMe lead to the values for the bond dissociation energy of Mo≡Mo and Mo≡C listed in Table 9, along with the enthalpy for the reaction in eqn 5.

The calculations suggest that the reductive cleavage by $Mo_2(OR)_6$ compounds may be enthalpically disfavored despite the notably weaker Mo−Mo bond strength. For $W_2(ER)_6$ compounds, the calculated difference between E = O and E = S cannot be viewed as significant.

The computed M-EH bond strength for the four compounds $M_2(EH)_6$ are also listed in Table 9. This clearly shows that D(M−O) > D(M−S) and also that D(W−E) > D(Mo-E). The latter is expected based on overlap arguments and the former supports the statement made previously that the M−O^{t}Bu bonds were enthalpically favored in the equilibrium reaction 4.

Concluding Remarks

^{t}BuO ligands are enthalpically favored over ^{t}BuS ligands in the M(3+) systems described in this work which contrasts to previous findings for the platinum group metals in their relative affinities for alkoxide and thiolate ligands. In the closely related series of compounds $W(E^tBu)_3(NO)(py)$ and $[Mo(E^tBu)_3(NO)]_2$, where E = O and S the values of ν(NO) are lower for E = O than for E = S. This parallels the finding of McCleverty and co-workers [32] who found for the series of compounds Mo(μ^3-HB(3.5-Me_2pz)(NO)(X)(Y) that ν(NO) was higher when X = SR relative to X = OR. As those authors suggested, we too ascribe this difference in ν(NO) as a relative measure of Mo dπ to NO π* back-bonding which is assisted by the relative π-donor properties of the ligands: $RO^- > RS^{\cdot -}$.

The DFT calculations on the hypothetical molecules $M_2(EH)_6$, $M(EH)_3(NO)(NH_3)$ and the fragments $M(EH)_3$ indicate that the M−O bonds are more polar than their M−S counterparts. The influence of $E_{p\pi}$ to $M_{d\pi}$ donation is seen in the relative energies of the M−M π orbitals, the population of N−O π* MO which mixes with the filled M(d_{xz},d_{yz}) orbitals, and the relative ordering and absolute energies of metal (d_{xz},d_{yz}) and d_{z^2} orbitals in the $M(EH)_3$ fragments. The estimates of the M−M triple bond strengths reveal that the Mo−Mo triple bond is roughly two-thirds as strong as the W−W triple bond, a ratio that parallels the bond strengths of the metals in their metallic state. D(M−M) in the $M_2(EH)_6$ molecules, differs by 12 kcal/mol for W and 6 for Mo for E = OH and SH. Calculations of the strength of the M−C triple bond strengths in $(HE)_3M{\equiv}CMe$ imply a similar trend, although the differences are even smaller. While we cannot rule out thermodynamics as a contributing factor to the lack of reactivity of W≡W bonded complexes supported by thiolate ligands toward π-acceptor ligands such as CO, alkynes, and nitriles, we are of the opinion that kinetic factors associated with the frontier MO's of the W_2^{6+} unit are more important. The alkoxide ligands raise the dπ-orbitals on the metal and thereby labilize the dinuclear center toward the uptake of π-acid ligands, a necessary step prior to reductive cleavage if this is favored on enthalpic grounds, and the prerequisite for adduct formation of the type $M_2(EH)_6(\mu$-X), where X = CO, RCCR or RCN.

How does this study relate to the general questions raised in the Introduction? Because of orbital energies it is clear that thiolates are more covalently bonded to metals in their lower and middle oxidation states. They are good σ-donors and moderate π-donors. By comparison alkoxides have more polar or ionic bonds but are stronger π-donors. For early transition metals with vacant d_π orbitals this will lead to stronger M-OR bonds relative to M-SR bonds. Also for metals in high oxidation states where the metals are oxidizing, OR will be greatly favored over SR as the latter can readily be oxidized by charge transfer from the sulfur lone-pair to the metal. The latter is akin to the relative stability of metal halogen complexes such as MoF_6 and $MoCl_6$. [The latter is unstable with respect to formation $MoCl_5$ and Cl_2 wherein the metal is reduced and Cl^- is oxidized.]

(32) McCleverty, J. A. *Chem. Soc. Rev.* **1983**, *12*, 331.

Table 8. Comparison of the Frontier Orbital Energies (eV) and Symmetries for the $W(EH)_3((NO)(NH_3)$ Molecules, Where E = O and S, Using Gaussian B3LYP CEP-121G with Polarization Added for O and S and the CEP Effective Core Potential

	LUMO/SLUMO	HOMO/SHOMO	3rd HOMO	4th/5th HOMO
$W(OH)_3(NO)(NH_3)$	E, −0.83 eV	E, −5.84 eV	A_2, −8.58 eV	E, −8.96 eV
$W(SH)_3(NO)(NH_3)$	E, −.09 V	E, −6.49 eV	A_2, −6.90 eV	E, −7.67 eV

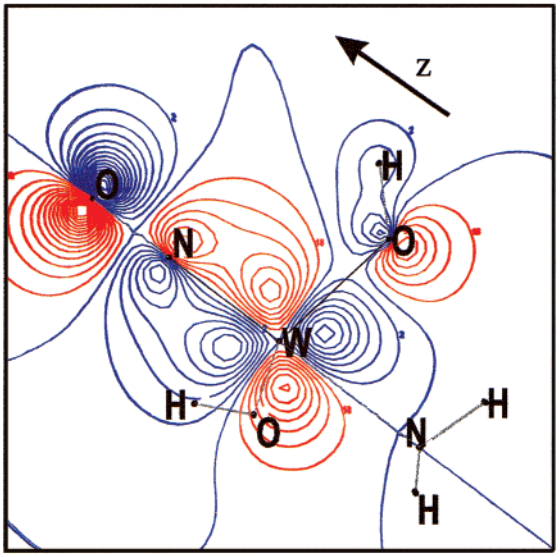

Figure 11. HOMO of $W(OH)_3(NO)(NH_3)$ showing the Wd_π-to-NO π^* bonding and the influence of O p_π bonding.

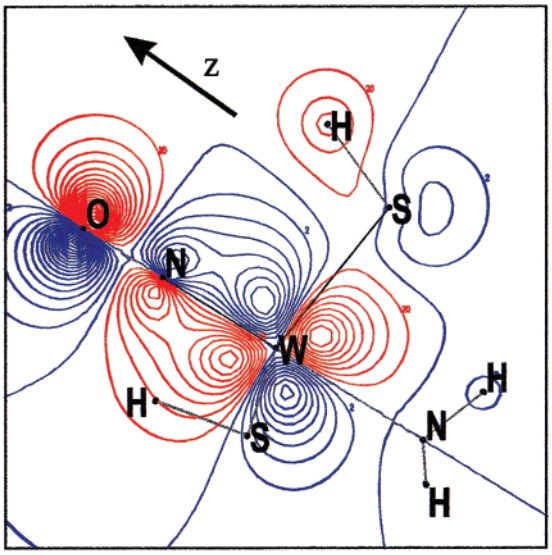

Figure 12. HOMO of the $W(SH)_3(NO)(NH_3)$ molecule showing the Wd_π-to-NO π^* bonding and S participation.

These comparisons can be generalized by a simple orbital interaction diagram of the type shown in Figure 15, where the frontier orbitals are shown for the formation of a bent M−E-H fragment. For simplicity the M−E-H angle is taken to be ca. 120° for both E = O and S and only two d orbitals are used, namely the dσ and one dπ orbital.

The diagram (Figure 15) shows how the M−S σ bond is more covalent while the M−O σ bond has significant ionic character since it is largely a stabilized oxygen sp^2 hybrid orbital. With a M−E-H angle of 120° the sulfur lone-pair lies at a significantly lower binding energy than its oxygen counterpart. As we have seen for $M_2(SH)_6$ molecules this is at ca. 7 eV which is close in energy or even higher (lower binding energy) than the metal valence d orbitals.

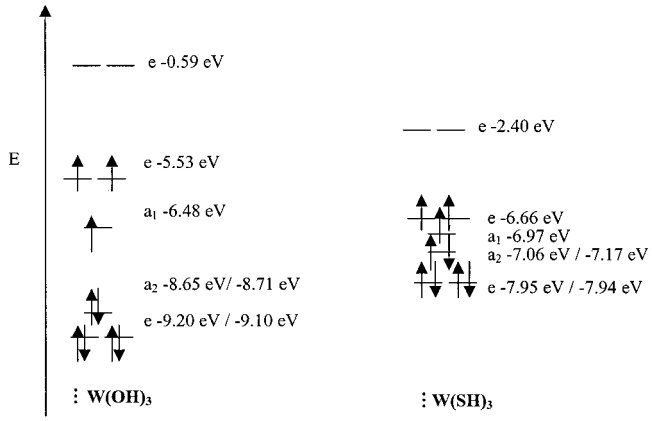

Figure 13. An orbital energy level diagram comparing the frontier molecular orbital energies $W(EH)_3$, where E = O and S. The two energies correspond to α and β electronic energies.

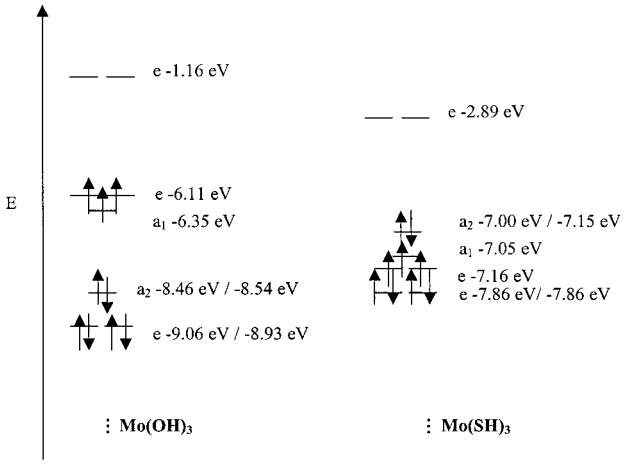

Figure 14. An orbital energy level diagram comparing the frontier molecular orbital energies $Mo(EH)_3$, where E = O and S. The two energies correspond to α and β electronic energies.

The effect of π-donation, which is greater for oxygen, raises the energy of the metal based dπ orbitals. In the case of filled dπ electrons on the metal this gives rise to a full blown π^* orbital occupancy. This filled-filled orbital interaction will weaken M-OR bonds more than M-SR bonds. In this way one can readily see why for the later transition metals, such as in the complexes of Ru(II) and Ni(II) discussed in the Introduction, the M-SR bonds are enthalpically favored.

In the presence of metal ions with partially filled dπ orbitals there will be selective modes of bonding for both SR and OR ligands wherein the M−E π-donation avoids the use of the filled dπ orbitals. In the presence of π-acceptor ligands the latter will be stabilized by back-bonding M dπ to Lπ.* Finally, in the case where the E pπ to M dπ orbital interaction is fully repulsive the higher lying M dπ orbitals will be best stabilized by the presence of a π-acceptor which allows for a ligand-to-ligand π-donation through the metal center as depicted by II. The maximum through metal ligand-to- ligand π-donation is favored when the π-donor and π-acceptor are mutually trans.

Table 9. Values for the M≡M Bond Strength in Various M_2L_6 Compounds, M≡C Bond Strength in $(HE)_3MCMe$ Compounds, M−E Bond Strength in $M_2(EH)_6$ Compounds, and the ΔH Value for the Reaction $M_2(EH)_6 + MeC{\equiv}CMe \rightarrow 2(HE)_3MCMe$

	kcal/mol	ref		kcal/mol	ref
$Mo_2(NMe_2)_6$	48	24	$(HO)_3WCMe$	136	c
$W_2(NMe_2)_6$	81	24	$(HS)_3WCMe$	129	c
Mo_2H_6	68	25a	$Mo_2(OH)_6$, Mo−O	97	*c*, *d*
$Mo_2(OH)_6$	62	25b	Mo2(SH)6, Mo−S	71	*c*, *d*
$W_2(OH)_6$	86	25b	$W_2(OH)_6$, W−O	121	*c*, *d*
$Mo_2(OH)_6$	62	c	$W_2(SH)_6$, W−S	79	*c*, *d*
$Mo_2(SH)_6$	55	c	ΔH, M = Mo, E = O	10.9	c
$W_2(OH)_6$	91	c	ΔH, M = Mo, E = S	7.6	c
$W_2(SH)_6$	79	c	ΔH, M = W, E = O	−0.6	c
$(HO)_3MoCMe$	116	c	ΔH, M = W, E = S	1.6	c
$(HS)_3MoCMe$	114	c			

[c] This work, using Gaussian B3LYP CEP-121G with polarization added for O and S and the CEP effective core potential. [d] These values are the first M−E dissociation energy defined as the ΔE of the $\bullet M(EH)_5$ and $EH\bullet$ fragments and the $M_2(EH)_6$ molecule.

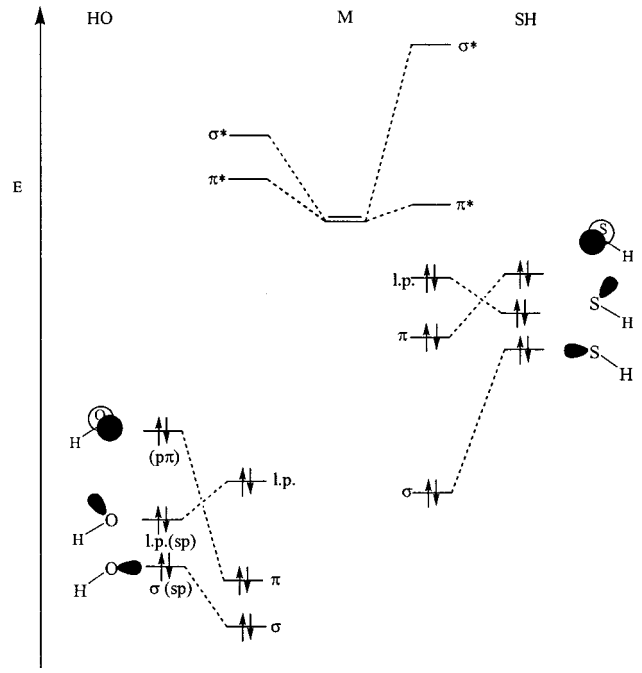

Figure 15. Schematic MO energy level diagram comparing the formation of M−EH bonds, where E = O and S.

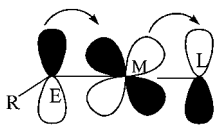

II

For the complexes $(RE)_3M{\equiv}M(ER)_3$, the containment of the M−E-H planes in D_{3d} symmetry with the M−M axis within the M−E-H planes minimizes filled-filled ligand−metal dπ interactions and allows maximum M−M and M−L π bonding. However, as the M−E-C angle increases from 120° and as the M−M-E angle increases from 90°, the repulsive ligand to metal π-bonding becomes more important. The larger M−O−C angles (relative to M−S−C angles) undoubtedly account for a significant part of the raising in energy of the filled metal dπ type orbitals, which in $M_2(OR)_6$ are the M−M π bonding MO's.

For the nitrosyl complexes discussed in this work a similar situation pertains. With C_{3v} symmetry and the M−E-C planes bisecting along the *z* axis, ligand to metal π-donation uses principally the metal d_{xy} and $d_{x^2-y^2}$ orbitals. However, as the (nitrosyl)N−M-E angle increases from 90° and as the M−E-C angle becomes more obtuse so now do the metal d_{xz} and d_{yz} orbitals become involved. It is again this involvement which is favored for the alkoxides over the thiolates and which leads to enhanced back-bonding to the nitrosyl ligand. Thus, the bonding in $M_2(EH)_6$ compounds and $W(EH)_3(NO)(NH_3)$ serve to illustrate the general properties of alkoxide and thiolate ligand bonding in transition metal chemistry.

Experimental Section

All manipulations were carried out under an inert atmosphere of oxygen-free UHP-grade argon using standard Schlenk techniques or under a dry and oxygen-free atmosphere of nitrogen in a Vacuum Atmospheres Co. Dry Lab system. Benzene, toluene, and hexane were distilled from sodium and benzophenone and degassed and stored over 4 Å sieves. *tert*-Butyl thiol was distilled from calcium hydride under argon prior to use. Nitric oxide was used as received. Toluene-d_8 and benzene-d_6 were degassed and stored over 4 Å sieves for 24 h before use. $W_2(O^tBu)_6$,[33] $Mo_2(O^tBu)_6$,[26] $W_2(O^tBu)_6(\mu\text{-CO})$,[13] $W(O^tBu)_3(NO)(py)$,[14] and $[Mo(O^tBu)_3NO]_2$[15] were prepared according to literature procedures. Infrared spectra were collected on a Nicolet 510P FT-IR spectrophotometer as KBr pellets. ^1H and ^{13}C NMR spectra were collected on a Gemini-300 300 MHz spectrometer or on a Varian 400 MHz spectrometer in dry and oxygen-free benzene-d_6 and toluene-d_8. The ^1H NMR chemical shifts are in parts per million relative to the C_6D_5H singlet at 7.16 ppm or the methyl protio impurity of toluene at 2.09 ppm. The ^{13}C NMR chemical shifts are in parts per million relative to the C_6D_6 triplet at 128 ppm or the toluene methyl septet at 20.4 ppm. Elemental analyses were done with a Perkin-Elmer 2400 C, H, N/S elemental analyzer.

Preparation of $W_2(O^tBu)_2(S^tBu)_4$. $W_2(O^tBu)_6$ (2.0 g, 2.5 mmol) was dissolved in benzene (50 mL) in a 100 mL Schlenk flask to give a red solution. ^{t}BuSH (4.2 mL) was slowly added via syringe. After 2 days, the solvent, excess ^{t}BuSH, and ^{t}BuOH were removed under reduced pressure. By ^1H NMR, the product contained 85% $W_2(O^tBu)_2(S^tBu)_4$ and 15% $W_2(O^tBu)_3(S^tBu)_3$. The product was redissolved in benzene, and ^{t}BuSH (2.5 mL) was added. After 2 days, the volatile components were removed under reduced pressure, affording a red powder, $W_2(O^tBu)_2(S^tBu)_4$, which was recrystallized from hexanes (1.9 g, 88% yield). Anal. Calcd for $W_2(O^tBu)_2(S^tBu)_4$: C, 33.11; H, 6.25. Found: C, 32.70; H, 6.31. ^1H NMR (toluene-d_8, 20 °C, 300 MHz): 1.43 ppm (36 H), 1.97 ppm (18 H). $^{13}C\{^1H\}$ NMR (toluene-d_8, 20 °C, 75 MHz): 32.3 ppm $OC(CH_3)_3$, 36.3 ppm $SC(CH_3)_3$, 48.3 ppm $SC(CH_3)_3$, 86.2 ppm $OC(CH_3)_3$. IR (KBr pellet): 2970 (m), 2918 (m), 2890 (m), 2856 (m), 1453 (w), 1361 (m), 1155 (s), 981 (s), 796 (w).

Preparation of $Mo_2(O^tBu)_2(S^tBu)_4$. $Mo_2(O^tBu)_6$ (0.5 g, 0.79 mmol) was dissolved in benzene (30 mL) in a 50 mL Schlenk flask to give a red solution. ^{t}BuSH (1.8 mL) was slowly added via syringe. After 2 days, the solution was filtered through Celite to remove insoluble material. The volatile components were removed under reduced pressure. $Mo_2(O^tBu)_2(S^tBu)_4$, a red powder, was recrystallized from hexanes (0.3 g, 55% yield.) Anal. Calcd for $Mo_2(O^tBu)_2(S^tBu)_4$: C, 41.49; H, 7.83. Found: C, 40.79; H, 7.41. ^1H NMR (benzene-d_6, 20 °C, 300 MHz): 1.42 ppm (36 H), 1.92 ppm (18 H). $^{13}C\{^1H\}$ NMR (benzene-d_6, 20 °C, 75 MHz): 32.6 ppm $OC(CH_3)_3$, 36.1 ppm $SC(CH_3)_3$, 48.3 ppm $SC(CH_3)_3$, 84.5 ppm $OC(CH_3)_3$. IR (KBr pellet): 2968 (m), 2917 (m), 2890 (w), 2856 (w), 1453 (w), 1360 (m), 1156 (s), 981 (s), 793 (w).

Determination of Equilibrium Constants for the Reaction of $M_2(O^tBu)$ (M = Mo, W) with ^{t}BuSH. In a typical experiment, 15 mg of $M_2(O^tBu)_6$ (M = Mo, W) and 500 μL of toluene-d_8 were added to an NMR tube. A 10 equiv sample of ^{t}BuSH was vacuum-transferred to the NMR tube, which was then flame-sealed. The NMR tube was kept at constant temperature until equilibrium was reached. The relative areas of the peaks in the ^1H NMR spectra for $M_2(O^tBu)_6$, $M_2(O^tBu)_2(S^tBu)_4$,

(33) (a) Akiyama, M.; Chisholm, M. H.; Cotton, F. A.; Extine, M. W.; Haitko, D. A.; Little, D.; Fanwick, P. E. *Inorg. Chem.* **1979**, *18*, 2266. (b) Chisholm, M. H.; Cotton, F. A.; Murillo, C. A.; Reichert, W. W. *Inorg. Chem.* **1977**, *16*, 1659.

^{t}BuOH, and ^{t}BuSH were used to determine the concentrations of the species and to calculate the equilibrium constant of the reaction. For M = W, $K = 1.6 \times 10^{-2}$ at 272 K and 1.9×10^{-3} at 289 K.

For M = Mo, $K = 5.7 \times 10^{-2}$ at 272 K, 9.9×10^{-4} at 289 K, and 4.5×10^{-5} at 299 K.

Reaction of $W_2(O^tBu)_2(S^tBu)_4$ with ^{13}CO and ^{t}BuCCH. In a typical experiment, 15 mg of $W_2(O^tBu)_2(S^tBu)_4$ was dissolved in 500 μL of toluene-d_8 in a Rototite NMR tube. A 1 equiv sample of the organic reagent was then added. The reaction was monitored over several days by ^{1}H and ^{13}C{^{1}H} NMR spectra, and for each case no evidence of reaction was observed.

Reaction of $W_2(O^tBu)_2(S^tBu)_4$ with Me^{13}CN. A 16 mg sample of $W_2(O^tBu)_2(S^tBu)_4$ was dissolved in 500 μL of toluene-d_8. A 10 equiv sample of Me^{13}CN was added via microsyringe. The ^{1}H and ^{13}C{^{1}H}-NMR spectra were monitored from +50 to −80 °C to look for low-temperature adduct formation. There was no evidence of cleavage products or adduct formation at any temperature.

Reaction of $W_2(O^tBu)_2(S^tBu)_4$ with PhCN. A 20 mg sample of $W_2(O^tBu)_2(S^tBu)_4$ was dissolved in 500 μL of toluene-d_8. A 10 equiv sample of PhCN was added via microsyringe. The ^{1}H MNR spectra were monitored over 24 h to look for cleavage products. There was no evidence of cleavage products or any other reaction.

Reaction of $W_2(O^tBu)_2(S^tBu)_4$ with $^{13}CO_2$. A 20 mg sample of $W_2(O^tBu)_2(S^tBu)_4$ was dissolved in 500 μL of toluene-d_8. A 6 equiv sample of $^{13}CO_2$ was condensed into the NMR tube, by use of a calibrated gas line. No evidence of reaction was observed by ^{1}H and ^{13}C {^{1}H}NMR spectroscopy.

Reaction of $W_2(O^tBu)_6(\mu$-CO) with ^{t}BuSH. A 20 mg sample of $W_2(O^tBu)_6(\mu$-CO) was dissolved in benzene-d_6 in an NMR tube. Excess ^{t}BuSH (10 equiv) was added to the NMR tube via vacuum transfer. ^{1}H and ^{13}C{^{1}H} NMR spectroscopy revealed the presence of free CO, $W_2(O^tBu)_6$, $W_2(O^tBu)_5(S^tBu)$, $W_2(O^tBu)_4(S^tBu)_2$, $W_2(O^tBu)_3(S^tBu)_3$, and $W_2(O^tBu)_2(S^tBu)_4$ over several hours.

Preparation of $W(S^tBu)_3(NO)(py)$. $W(O^tBu)_3(NO)(py)$ (0.23 g, 0.45 mmol) was dissolved in toluene (10 mL). A 10 equiv sample of ^{t}BuSH (0.5 mL) was slowly added via syringe. The yellow solution was allowed to stir for 12 h. The volatile components were removed under reduced pressure, yielding $W(S^tBu)_3(NO)(py)$ as a yellow powder. The product was then recrystallized from toluene, yielding yellow X-ray-quality crystals (0.19 g, 76% yield.) Anal. Calcd for $W(S^tBu)_3(NO)$-(py): C, 36.43; H, 5.75; N, 5.00. Found: C, 36.51; H, 5.68; N, 5.11. ^{1}H NMR (toluene-d_8, 22 °C, 300 MHz): 1.88 ppm. ^{13}C{^{1}H} NMR (toluene-d_8, 22 °C, 75 MHz): 36.0 ppm (SC(CH_3)$_3$), 53.2 ppm (S*C*(CH_3)$_3$). IR (KBr pellet): 2963 (w), 2916 (m), 1604 (s), 1444 (w), 1348 (w), 1251 (s), 1095 (s), 1021 (s), 796 (s), 691 (m), 606 (w), 563 (w).

Preparation of $[Mo(S^tBu)_3NO]_2$. $[Mo(O^tBu)_3NO]_2$ (0.45 g, 0.65 mmol) was dissolved in toluene (20 mL). A 10 equiv sample of ^{t}BuSH (0.7 mL) was slowly added. The volatile components were removed under reduced pressure after the reaction had been stirred for 12 h, giving a yellow powder. The product, $[Mo(S^tBu)_3NO]_2$, was recrystallized from toluene, yielding yellow X-ray-quality crystals (0.32 g, 63% yield). Anal. Calcd for $[Mo(S^tBu)_3NO]_2$: C, 36.63; H, 6.91; N, 3.56. Found: C, 36.68: H, 6.83; N, 3.66. ^{1}H NMR (toluene-d_8, 20 °C, 300 MHz): 1.72 ppm (terminal, 36 H), 2.00 ppm (bridging, 18 H). ^{13}C-{^{1}H} NMR (toluene-d_8, 20 °C, 75 MHz): 35.0 ppm (SC(CH_3)$_3$, bridging), 60.2 ppm (S*C*(CH_3)$_3$, bridging) 35.1 ppm (SC(CH_3)$_3$, terminal), 55.3 ppm (S*C*(CH_3)$_3$, terminal). IR (KBr pellet): 2963 (w), 2919 (w), 2892 (w), 2874 (w), 1644 (s), 1454 (m), 1389 (m), 1363 (m), 1148 (m), 1021 (w), 803 (w), 611 (w), 552 (w), 435 (w).

^{1}H NMR data for $W_2(O^tBu)_{6-n}(S^tBu)_n$ in benzene-d_6, 22 °C, δ (ppm): $n = 0$, 1.63; $n = 1$, 1.61 (3 ^{t}BuO), 1.78 (2 ^{t}BuO), 1.40 (1 ^{t}BuS); $n = 2$, 1.71 (4 ^{t}BuO), 1.41 (2 ^{t}BuS); $n = 3$, 1.85 (2 ^{t}BuO), 1.83 (1 ^{t}BuO), 1.49 (2 ^{t}BuS), 1.32 (1 ^{t}BuS); $n = 4$, 1.97 (2 ^{t}BuO), 1.43 (4 ^{t}BuS).

^{1}H NMR data for $Mo_2(O^tBu)_{6-n}(S^tBu)_n$ in benzene-d_6, 22 °C, δ (ppm): $n = 0$, 1.64; $n = 1$, 1.52 (3 ^{t}BuO), 1.71 (2 ^{t}BuO), 1.31 (1 ^{t}BuS); $n = 2$, 1,1-isomer, 1.56 (3 ^{t}BuO), 1.87 (1 ^{t}BuO), 1.42 (2 ^{t}BuS); $n = 2$, 1,2-isomer, 1.67 (4 ^{t}BuO), 1.30 (2 ^{t}BuS); $n = 3$, 1.85 (1 ^{t}BuO), 1.81 (2 ^{t}BuO), 1.41 (2 ^{t}BuS), 1.25 (1 ^{t}BuS); $n = 4$, 1.88 (2 ^{t}BuO), 1.34 (4 ^{t}BuS).

Table 10. Summary of Crystallographic Data for $W_2(O^tBu)_2(S^tBu)_4$, $W(S^tBu)_3(NO)(py)$, and $[Mo(S^tBu)_3NO]_2$

empirical formula	$W_2C_{24}H_{72}S_4O_2$	$C_{17}H_{32}N_2OS_3W$	$C_{24}H_{54}N_2O_2S_6Mo_2$
fw	870.63	560.49	768.98
space group	$P2_1/a$	$I42d$	$I42d$
unit cell params			
a, Å	17.666(3)	15.8723(6)	12.288(1)
b, Å	11.488(3)	15.8723(6)	12.288(1)
c, Å	18.548(3)	36.447(2)	48.707(4)
α, deg		90	
β, deg	117.00	90	
γ, deg		90	
V, Å^{-3}	3353.84	9182.2(7)	7354.00
Z	4	16	8
d_{calcd}, g cm^{-1}	1.724	1.622	1.422
cryst size, mm	0.12 × 0.10 × 0.10	0.68 × 0.48 ×0.41	0.30 × 0.30 × 0.30
λ (Å)	0.71069	0.71073	0.71073
μ (cm^{-1})	72.596	53.18	10.438
$R(F)$	0.0791	0.0418	0.0266
$R_w(F)$	0.0782	0.1175	0.0228

Single-Crystal X-ray Determinations. General operating procedures and a listing of programs employed have been previously given.[34] A summary of crystal data is given in Table 10. Further information is given in the Supporting Information and is available from the Cambridge Crstallographic Data Center.

Computational Procedures for the Elucidation of Electronic Structure. As an initial geometry in the calculations, the structural parameters associated with known $M_2(ER)_6$ compounds were employed in the $M_2(EH)_6$ molecules (E = O, S) where the E−H bond replaced the E−C bond of the alkyl or aryl group. The parameters for the $W_2(O^t$-$Bu)_2(S^tBu)_4$ reported here were used as the starting geometry for the $M_2(OH)_2(SH)_4$ compounds, and the central $W(EC)_3(NO)(N)$ parameters were taken from the $W(E^tBu)_3(NO)(py)$ structure for the calculations of $W(EH)_3(NO)(NH_3)$. In all cases, the geometries were optimized.

For all the Gaussian 98[21] calculations the B3LYP[19] method was used. The first calculations were done with LANL2DZ[20] as the basis set with the default grid.

Calculations were also done at the triple-zeta level with polarization functions added for oxygen and sulfur. The basis sets used were CEP-121G[22] with polarization functions added for oxygen and sulfur. The effective core potentials used with these basis sets were CEP and LANL2. In both cases, the metal *n*s, *n*p, (*n* + 1)s, and *n*d electrons were retained from the core and calculated explicitly.

Bond energies were calculated by the difference in energy of the original molecule and the fragments that result from homolytic cleavage of the bond of interest. The fragment geometries were optimized, and frequency calculations were performed to obtain energies at 298 K. The $M(EH)_3$ fragments were found to have a lower ground state with three unpaired electrons than with one unpaired electron, while for the CMe fragment the ground state was found to be a doublet.

Mulliken population analyses of individual molecular orbitals were obtained using MELD.[35]

Calculations were also done on $M_2(EH)_6$, $M(EH)_3$, MeC≡CMe, $(HE)_3$WCMe, and CMe using ADF 2000.[23] The atoms for these calculations were created using the basis sets in ZORA/IV which are triple-zeta and include polarization functions for O and S. Frozen core shells were used with up to 4d frozen for W, up to 3d frozen for Mo, 1s frozen for O and C, and 2p frozen for S. Relativistic core potentials were generated with DIRAC calculations. Molecular optimization was done with BLYP, and ZORA relativistic terms were used. Bond energies were calculated as described above, but in this case frequency calculations were not performed.

Orbital plots were made using Molden.[36]

(34) Chisholm, M. H.; Folting, K.; Huffman, J. C.; Kirkpatrick, C. C. *Inorg. Chem.* **1984**, *23*, 1021.

(35) MELD is a set of electronic structure programs written by L. E. McMurchie, S. T. Elbert, S.R Langhoff, and E. R. Davidson, with extensive modifications by D. Feller and D. C. Rawlings. Available from http://php.indiana.edu/~davidson/.

Acknowledgment. We thank the National Science Foundation for support of this work and Drs. T. Budzichowski and G. Gamma for preliminary investigations of the reaction between $W_2(O^tBu)_6$ and ^{t}BuSH. We also thank the reviewers for their constructive criticism of this work. This paper is dedicated to S. J. Lippard on the occasion of his 60th birthday.

Supporting Information Available: CIF data for $W_2(O^tBu)_2(S^tBu)_4$, $[Mo_2(S^tBu)_3NO]_2$, and $W(S^tBu)_3(NO)(py)$ together with contour plots of the frontier orbitals of $W_2(EH)_6$, $W_2(OH)_2(SH)_4$, and $W(EH)_3(NO)(NH_3)$ molecules and $W(EH)_3$ fragments where E = O and S, a comparison of the spin densities and energies of $M(OH)_3$ with one and three unpaired electrons, and a comparison of the orbital energy diagrams for $W_2(OH)_6$ and $W_2(SH)_6$ from the ADF 2000 calculations and tables comparing the bond energies obtained using the various calculations (print/PDF). This material is available free of charge via the Internet at http://pubs.acs.org

JA001208N

(36) Schaftenaar, G., Noordik, J. H. Molden: a pre- and post-processing program for molecular and electronic structures. *J. Comput.-Aided Mol. Des.* **2000**, 14, 123−134.